

**EURISOL- COMBINED CAVITATION DIAGNOSTICS**

RADE Ž. MILENKOVIĆ  
*Paul Scherrer Institut*  
*CH-5232 Villigen PSI, Switzerland*

and

SERGEJS DEMENTJEVS<sup>a</sup>, CYRIL KHAROUA<sup>b</sup>, KNUD THOMSEN<sup>a</sup>  
<sup>a</sup>*Paul Scherrer Institut, CH-5232 Villigen PSI, Switzerland*  
<sup>b</sup>*CERN-European Organization for Nuclear Research, Geneva, Switzerland*

**ABSTRACT**

An extensive experimental investigation has been carried out under project called EURISOL (The European Isotope Separation On-Line). The project was launched in 2005 by the European Union within the context of the 6th framework program for research development with the aim of developing a novel isotope production facility. As one of the milestones was to evaluate the detection of cavitation in liquid metal flows, two structural-hydraulic tests of the EURISOL neutron converter target mock-up, named METEX 1 and METEX 2 (MErcury Target EXperiment 1 and 2), have been conducted by PSI (Paul Scherrer Institut, Switzerland) in cooperation with IPUL (Institute of Physics of the University of Latvia, Latvia) and CERN (Conseil Européen pour la Recherche Nucléaire-European Organization for Nuclear Research). The methodology for cavitation detection was based on the advanced analysis of the structural acceleration, sound, pressure, strain and acoustic emission measurements. Namely, various advanced time-frequency analysis methods including the Short Time Fourier Transform (STFT), in particular, the Gabor Transform (GT) and the Discrete Wavelet Analysis (DWA) were applied on data samples with specified number of points. Even under noisy conditions, the detection of incipient cavitation was possible during carefully conducted transient tests. A special attention is given here to the following:

-Comparison of the experimental results obtained in METEX 1 experiment by two different techniques: acceleration sensors (AS), when the sensors must be attached to the structure and Laser Doppler Vibrometer (LDV), when the laser beam points at the structure.

-Analysis of the sound pressure data acquired by a microphone, which was located in the laboratory near the target.

The conclusions are also drawn about detection of cavitation performed by other experimental techniques employed during METEX 2 experiment i.e. acoustic emissions and high speed pressure measurements.

## **1. Introduction**

At the heart of the EURISOL facility, the liquid metal neutron converter target is designed to generate isotopes by fissioning uranium carbide arranged around it ([1],[2]). In a neutron spallation source, wherein a high-energy proton beam with high current impacts a heavy target material, the high volumetric heat-deposition level in the target window and material leads to the difficult task of maintaining the structural integrity of the hull and beam entrance window and keeping target temperatures within safe limits. There are essentially two possibilities to examine the thermal-hydraulic and structural behaviour of a high power liquid-metal target: i.e. a) to build and operate a full size target with adequate instrumentation for monitoring chosen parameters and to perform on-line and post-processing of the data; b) to simulate such a target by using up-to-date computational and finite element methods. As the design must be optimized and the safety issues have to be solved in advance before the target is operated, the target development must be based on numerical analysis as well as experimental work. Thus, the EURISOL development was based on the use of advanced

computational fluid dynamics and finite elements modelling. By using the codes design changes and their effects on flow development can be efficiently and consistently studied. At the end of the EURISOL design study, a prototype of the target was built and tested within relevant range of liquid metal flow rates.

Two structural-hydraulic tests of the EURISOL neutron converter target mock-up (Fig. 1), named METEX 1 and METEX 2 (MERcury Target EXperiment 1 and 2), were conducted by PSI in cooperation with IPUL (Institute of Physics of the University of Latvia, Latvia) and CERN (Conseil Européen pour la Recherche Nucléaire-European Organization for Nuclear Research) in December, 2008, January, 2009 and in March, 2009. The manufacture of the mock-up was the responsibility of PSI. The main goals of these tests were to investigate the structural and hydraulic behavior for various inlet flow conditions and for two geometrical configurations without and with flow vanes near the beam entrance window (BEW).

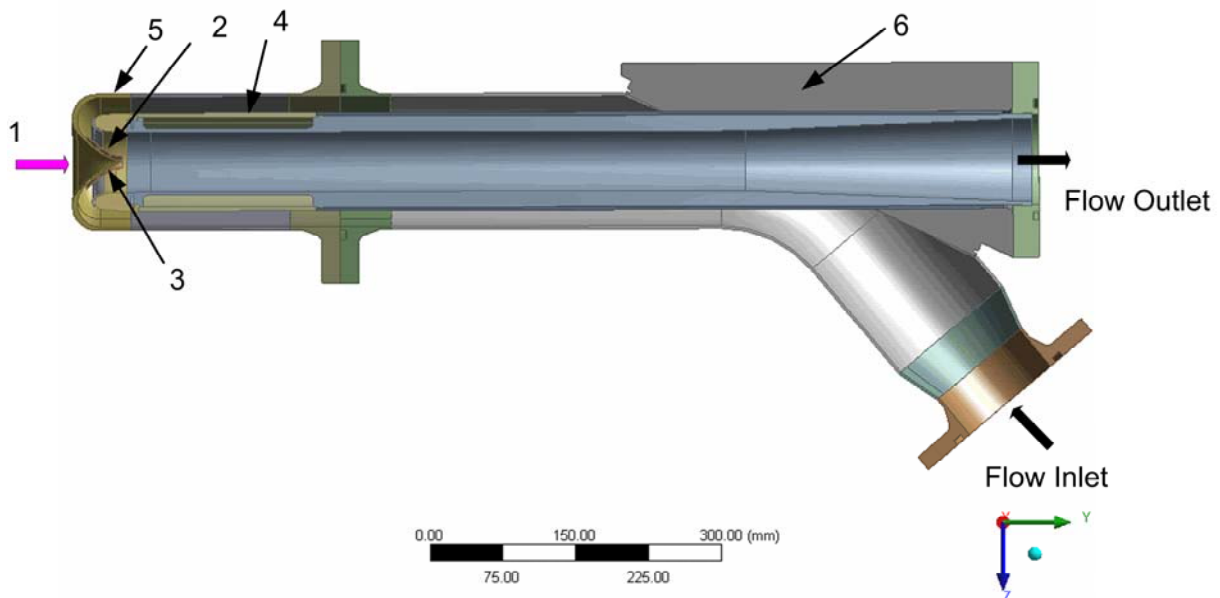


**Fig. 1.** Cross-section of the EURISOL converter target: 1 – proton beam; 2 – flow vanes; 3 – beam entrance window (BEW); 4 – guide tube (GT); 5 - target hull (TH); 6 – frame.

Since it is essential for the safety of the target to avoid cavitation during operation and as for liquid metal flows neither during hydraulic tests nor during real operational conditions any kind of visualization is possible, one of the milestones was to evaluate the detection of cavitation.

## 2. Data Analysis and Post-processing

Several advanced time–frequency analysis methods including the Discrete Wavelet Analysis (DWA) and, the Short-Time Fourier Transform (STFT) [3] were applied on collected data samples with specified numbers of points. The basic motivation for performing signal decomposition and quasi-thresholding in the wavelet space is to extract information about power distribution in the low-frequency sub-band and in high-frequency sub-band of the data. If consistently denoised signals are compared for various flow conditions classified

by varying one but fixing other characteristic non-dimensional numbers, for instance, typically for no flow, flow without cavitation, transient flow and developed cavitation, one may extract information on hidden coupled fluid–structure interactions. Therefore, the main objectives during current study were the following:

- to estimate reference system behavior for no flow and no cavitation;
- to detect incipient cavitation;
- to classify patterns in the time–frequency domain for different stages of cavitation.

### *2.1. Short-Time Fourier Transform*

As illustration of the Short-Time Fourier Transform (called also Windowed Fourier Transform), the spectrogram (Hanning window function was used here) of the analyzed acceleration signal is presented in Fig. 10. The STFT yields a complex matrix containing magnitude and phase for each point in time-frequency space, the so-called STFT coefficients. Depending on the size of the analysis window, which is fixed in the whole time domain, the signal can be represented either in good frequency or in good time resolution. As represented in Fig. 6, for the analysis of the acceleration signal with STFT a Hanning window with 512 samples, 64 frequency bins and 32 time steps was used. The total number of samples in all analyzed signals was  $2^{15} = 32768$ . This kind of representation reveals clearly some stationary components in the signal and shows why it is of interest to have high time resolution for the high-frequency contents or high frequency resolution for low-frequency contributions. The shorter time window allows identifying a precise time at which the signals change, but the precise frequencies are difficult to identify. At the other end of the scale, the longer time window allows the frequencies to be precisely seen. This property is related to the Heisenberg uncertainty principle. In our case a higher time resolution is necessary to detect high energy peaks, which are produced by collapsing bubbles as micro jets hit the structure.

### *2.2. Discrete Wavelet Analysis*

After application of DWA, which computes a single-level discrete wavelet transform using a 2-channel-analysis filter bank, the acceleration signal is decomposed into a low-frequency sub-band, and a high-frequency sub-band. The first represents so-called approximation coefficients (often called scaling coefficients), and the second represents so-called detailed coefficients (often called wavelet coefficients). Both sub-bands use half the sampling rate of the signal. This 2-channel Wavelet Analysis can be also referred to as 2-Level or 2-Wavelet Scales Decomposition. As the wavelets behave as a band-pass filter and the scaling function as a low-pass filter, the signal is correspondingly decomposed into two parts: low-frequency sub-band oscillations and high-frequency sub-band oscillations. In order to avoid a common misunderstanding, the low-frequency subband oscillations are here considered to be representing effects of large-scale disturbances on the solid structure, although that can be multi-scale effect. Similarly, the high-frequency sub-band oscillations are not considered to be confined to small scales, but may again be multi-scale, since their energy can be spread over all scales, like white noise. In case of cavitating flow, the high-frequency sub-band background oscillations, which are mainly generated by non-linear interactions between the fluid field and the walls, are strongly affected by the presence of collapsing bubbles. In case of no flow or flow without cavitation only interactions between turbulent structures and the walls exist, and, therefore, the signal patterns differ significantly as described in the next chapters. There are many mother wavelets used in practice. The choice of an appropriate mother wavelet depends on the information one needs to extract from the signal. We used Daubechies 14 wavelets, as they match well the bubble growth and collapse event shown in Fig. 10. We also denoised the signals in the wavelet space by applying the

same threshold on the wavelet coefficients. The signals were later reconstructed and compared in Fig. 8.

### 3. The Experiment

The final configuration chosen to solve the complex cooling requirements posed at the point of entry of the beam, the so-called beam window (see Fig. 1) led us to study and test the feasibility of using beam entrance window without and with integrated flow reverser i.e. thin flow vanes (see Fig. 1). Therefore, one of the main goals of experimental sessions METEX 1 and METEX 2 was to operate the EURISOL target mock-up under single-phase turbulent flow conditions, incipient and fully developed cavitation. The Cavitation number is defined as  $Ca = p_o - p_{sat}(t) / \Delta p$ , where  $\Delta p$  is the pressure loss,  $p_o$  is the pressure at the mock-up outlet and  $p_{sat}(t)$  is the saturation pressure of liquid metal vapor.

#### 3.1. Experimental Installation

All tests were conducted at the IPUL mercury loop (Fig. 2), which has DN100 piping assembled in a vertical plane on a frame. The target mock-up is connected to the loop interface flanges.

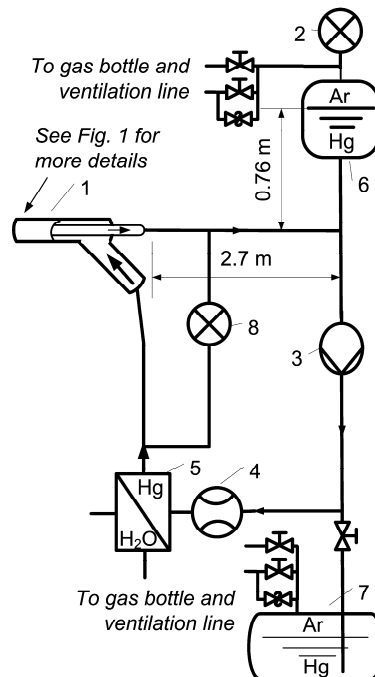


Fig. 2. Experimental set-up: 1—mock-up, 2—manometer-cover gas pressure, 3—electromagnetic pump, 4—flow meter, 5—heat exchanger, 6—expansion tank, 7—storage tank and 8—differential manometer-pressure loss measurement.

During the experiments reported here the pressure of the cover gas, the total mass flow rate, the pressure loss in the mock-up, temperatures at various locations, local static pressure, structural acceleration, strain and sound data were acquired at the most interesting locations (see [4] the experimental set-up is given in Fig. 2). The maximum liquid metal flow rate achieved with the configuration without and with flow vanes was between 10 and 11 l/s. As during the pump operation, up to 40kW of thermal power is dissipated into the liquid metal, four cooling water jackets on the stainless steel piping served to remove deposited heat. The

**ICANS XIX,**  
**19th Meeting on Collaboration of Advanced Neutron Sources**  
March 8 – 12, 2010  
Grindelwald, Switzerland

cooling water flow rate through all four heat exchangers was manually regulated. Therefore, the mercury temperature in the loop was kept in a range from 3 to 36 °C. The total mass of the mock-up filled with mercury was 176 kg.

### *3.2. Instrumentation*

The instrumentation used for hydraulic and structural test included the following:

- three acceleration sensors (KISTLER8632C5), which are fixed to the target mock-up as shown in Fig. 3. Structural acceleration of the target window was measured by CH0 (horizontal component) and CH1 (vertical component) and that of the target mock-up at the outlet interface flange by CH2 (vertical component of the acceleration);
- an ordinary microphone was used to acquire sound waves in the laboratory. The acoustic data are acquired by a personal computer at 22.5 kHz;
- a pressure sensor (KISTLER 601A, sensitivity 16 pC/bar, the scale was 1 pC/V i.e. 1bar=1V) was connected to an amplifier 5011B10 and attached to the BEW at the location presented in Fig. 3;
- an acoustic emission sensor (KISTLER 8152B, sensitivity 57 dBref 1V/(m/s)), was connected to coupler type 5125B and attached to the BEW at the location presented in Fig. 3;
- a Laser Doppler Vibrometer (LDV) was provided by CERN team [5]. The output of an LDV, a continuous analog voltage signal, was incorporated into the PSI data base. It is directly proportional to the structural velocity component along the direction of the laser beam. The laser beam was pointed at the center and at the side of the BEW;
- strain gauges attached to the hull at points designed to monitor bending of the hull in the vertical and horizontal planes as well as two points on each side of the critical weld connection from the hull to the support (Fig. 4);
- a conduction-type electromagnetic flow meter (calibrated with a Venturi tube) was used for measuring the liquid metal flow rate. The maximal error was 3% of the maximum flow rate;
- a differential manometer (YOKOGAWAEJA110, position 8 in Fig. 2) was used to measure the hydraulic pressure loss in the target mock-up. The maximal error was about 2% of the full range (2.5bar);
- a manometer (WIKAUT10, position 2 in Fig. 2) was used to measure the pressure of the cover gas in the system. The static pressure in the system could be adjusted in the range from 1 to 6.5 bar. The minimum static pressure in the system was 1bar due to the height difference of approximately 0.76m between the mercury level in the expansion tank and the target mock-up;

The acceleration, pressure, flow rate and pressure loss data were acquired by using both low-speed (National Instruments FIELDPOINT blocks, at 1Sample/s) and high-speed (Digital LeCroy Oscilloscope, at 5000Samples/s) data acquisition systems. They were collected into a single data base. Sound data are acquired by a personal computer at 22.5kHz. The strain data were acquired at 300 and 1200 Hz by SPIDER 8 system (HMB-Hottinger Baldwin

Messtechnik) into the different data base

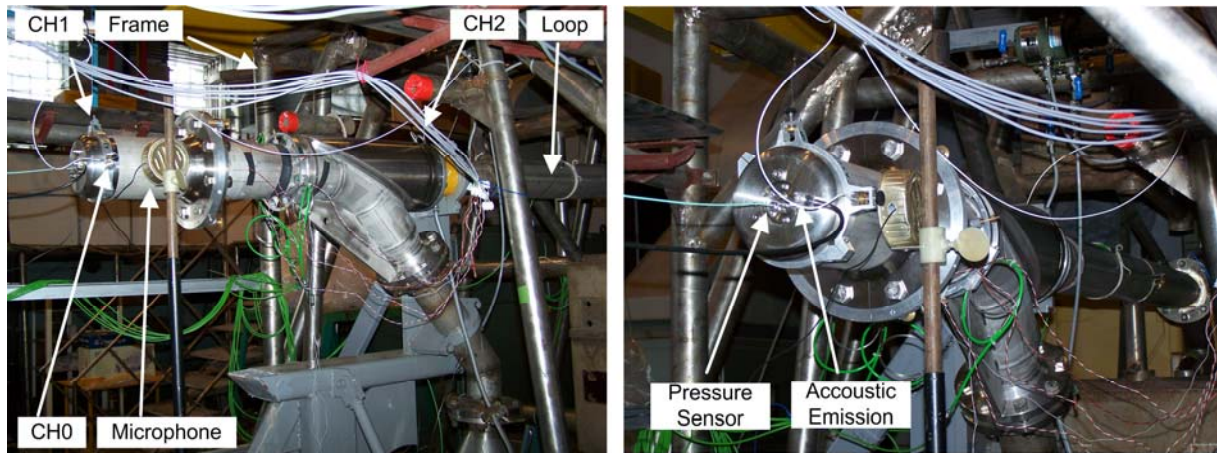


Fig. 3. Eurisol target mock-up equipped with sensors was connected to the IPUL liquid metal loop.

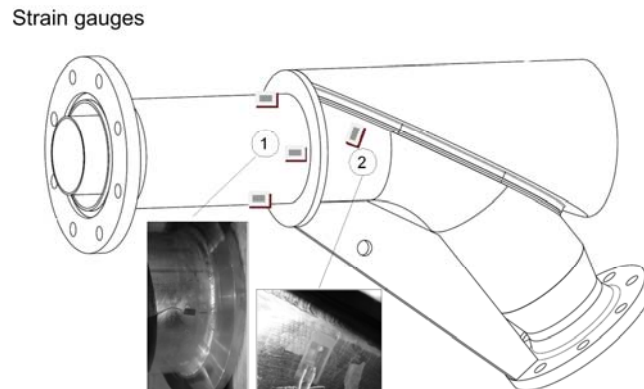


Fig. 4. Eurisol target mock-up equipped with the strain gauges.

### 3.3. Test Conditions

Extensive experimental campaign of the EURISOL mock-up target was separated into two sessions METEX 1 and METEX 2. After first results on cavitation detection were obtained during experimental session called METEX 1, the adopted BEW equipped with pressure and acoustic emission sensors was produced at PSI. Unfortunately, during METEX 2 session unexpected electromagnetic noise starting at 50 Hz with sub-harmonics at each additional 100 Hz affected high speed pressure measurements. Nevertheless, with the help of filtering techniques, the data were adopted for comparison with LES computational studies (as this was one of the objectives as well).

Some unique state-of-the-art results are summarized in the next two sections. It is demonstrated that it is possible to detect consistently incipient and fully developed cavitation in fully developed turbulent liquid metal flow with various sensors. Special attention is given to the sound and LDV data as these techniques can be remotely installed from hazardous regions and sources. In addition, all sensors listed in Chapter 3 can be successfully used for system health monitoring.

## 4. Results and Discussions

### 4.1. Highlights of METEX 1 Experimental Session

The variation of the liquid metal flow rate, the pressure loss and the pressure of the gas in the expansion tank are presented in Fig. 5 during 23.01.2009. Temperatures at the inlet and at the outlet of the mock-up were between 25 and 27 °C. In order to analyze efficiently the huge amount of acceleration (acquired at a sampling rate of 5000 Hz during 2 s), strain (acquired at 1200Hz during 10 minutes), LDV (acquired at 512 kHz during about 16 s) and sound data (acquired at 22.5 kHz during 60 s), the complete experimental data base was divided into several blocks, which are separately analyzed. During this unique transient test the pressure of the cover gas was reduced, whereas the pump was operated at the constant power (i.e. the flow rate at its maximum was kept constant). At about 13:33:07 the total pressure loss increased by about 200 mbar, whereas the flow rate slightly dropped (see Fig. 5). This event can be caused by intensive developed cavitation. Under such extreme conditions, the mock-up was operated over less than 1 minute. Afterwards the pressure of the cover gas was increased to about 4400 mbar. All data referred here are collected during METEX 1 session.

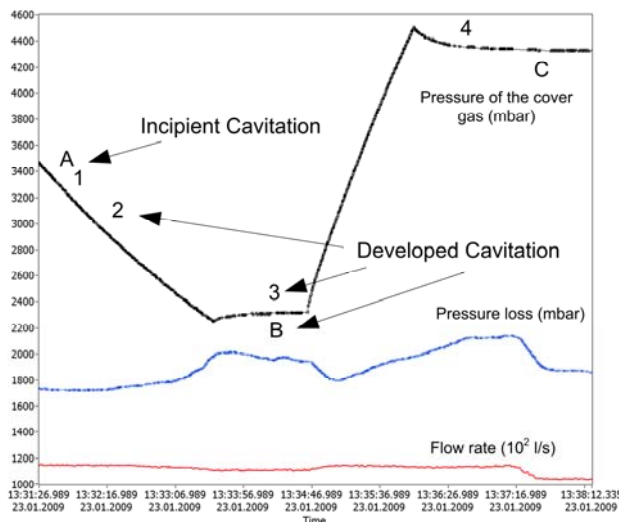


Fig. 5. Pressure of the cover gas, flow rate and total pressure loss in the mock-up during transient test. Regimes A, B and C refer to different flow regimes associated with the acceleration data, whereas the regimes marked as 1, 2, 3 and 4 refer to sound pressure data.

#### 4.1.1. Structural Acceleration

Acceleration data sampled from all three sensors and re-sampled LDV data, which are collected into a single data based, are shown in Fig. 6. The variation of amplitudes can be followed and representative data sets can be deduced and further analyzed. Significant enhancement of the structural acceleration amplitudes during pressure reduction is clear sign that developed cavitation took place (see Fig. 6). Even though, it was desirable to have consistent LDV and acceleration data, which would have meant to sample at the same frequencies, during this test it was decided to sample LDV data at much higher sampling rate and write them into different data base in order to catch fast incipient cavitation events. The LDV data written into the PSI data base were practically re-sampled at lower sampling rate the same as for acceleration data. Anyway, the results shown in Fig. 7 are remarkable. The RMS-values for regimes A and C are almost the same whereas for regime B, i.e. for fully developed cavitation the RMS-values are much higher. Instead of plotting flow rates and pressure of the cover gas, all data are scaled with the Cavitation number. It can be easily seen

**ICANS XIX,**  
**19th Meeting on Collaboration of Advanced Neutron Sources**  
 March 8 – 12, 2010  
 Grindelwald, Switzerland

that the cavitation starts at  $Ca=2.35$  (letter T in Fig. 7). This kind of representation may have remarkable practical importance, since no high computational power is needed for calculating the Cavitation number and the signal RMS. Additional question to be asked is: can we detect single events during transitional regimes? Hidden transient system behavior, which carries information about collapsing of first bubbles, was deduced from accompanying noise by using advanced time-frequency post processing methods.

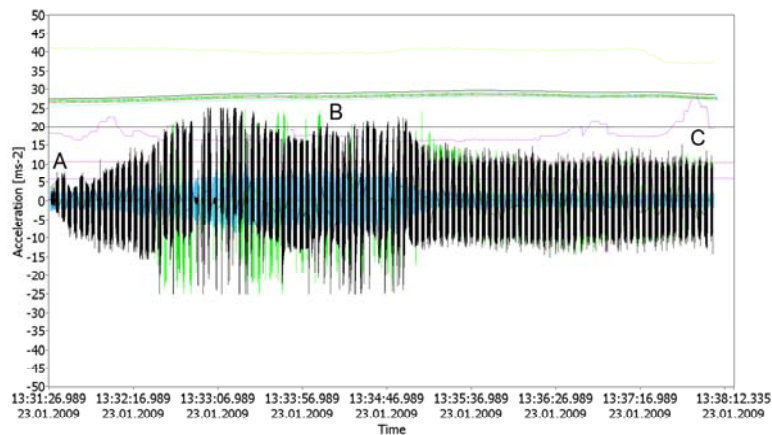


Fig. 6. Structural acceleration data sets (CH0, CH1 and CH2) and re-sampled LDV data set as written into the data base during the transient test explained above. The characteristic data sets A, B and C are analyzed in more details and the results are extensively discussed.

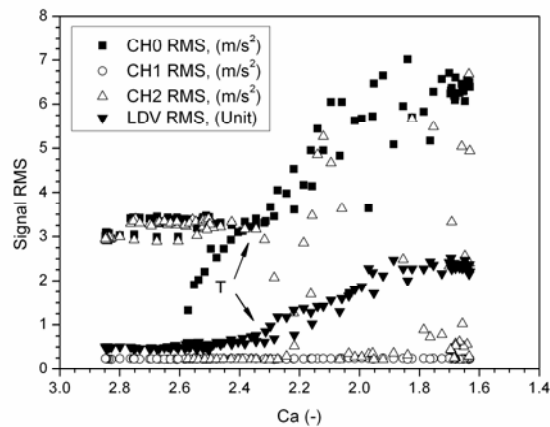


Fig. 7. rms- values of the acceleration data form three acceleration sensors and LDV as a function of the Cavitation number.

In order to follow the cause of events, three characteristic data sets, marked here as A (pre-cavitation regime), B (developed cavitation regime), and C (post-cavitation regime) are fully analyzed. The flow parameters (Fig. 5) are summarized here:  
 A:  $p_0 = 4457.35 \text{ mbar}$ ;  $Q = 11.46 \text{ l/s}$ ;  $Ca = 2.57$ ; started at 13:31:28;  
 B:  $p_0 = 3278.37 \text{ mbar}$ ;  $Q = 11.06 \text{ l/s}$ ;  $Ca = 1.69$ ; started at 13:37:57;  
 C:  $p_0 = 5332.39 \text{ mbar}$ ;  $Q = 10.38 \text{ l/s}$ ;  $Ca = 2.84$ ; started at 13:34:16.

**ICANS XIX,**  
**19th Meeting on Collaboration of Advanced Neutron Sources**  
 March 8 – 12, 2010  
 Grindelwald, Switzerland

Discrete Wavelet Transform with Daubechies 14 wavelets was used to denoise single events from data set A. The same threshold was used for all data sets. After thresholding in the wavelet space, the signals were reconstructed and compared. The incipient cavitation events, which correspond to the peaks clearly shown in (Fig. 8, first signal) are described in detail and zoomed in Fig. 9. In addition, Fig. 8 compares denoised signals with the same threshold values for three representative flow regimes. Thresholded signal for developed cavitation regime defers significantly from other signals.

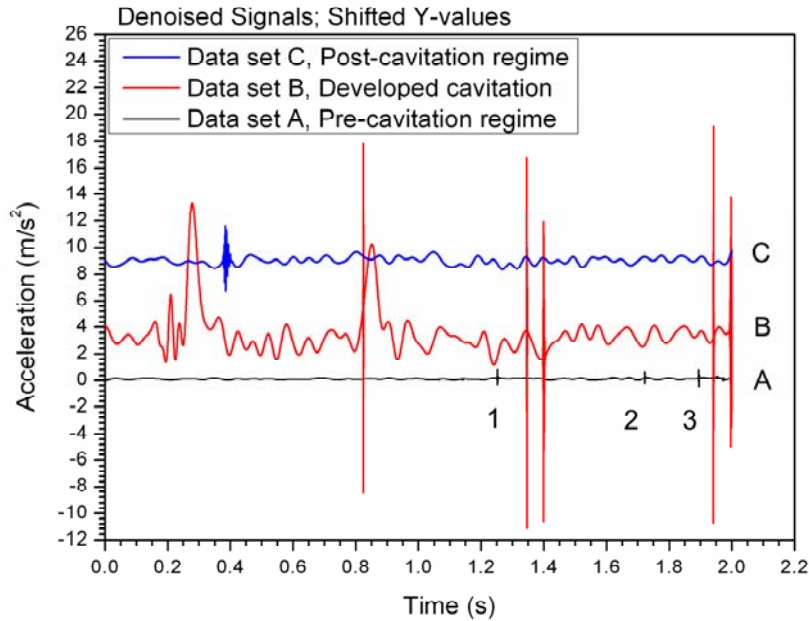


Fig. 8. Denoised signals for three characteristic regimes reveal incipient cavitation events in the data set A (events are notified by numbers 1, 2 and 3), as well as significant back ground noise enhancement due to the developed cavitation (data set B). Higher level noise is captured in data set C as in data set A. The amplitude values are shifted on the Y-axis in order to compare more easily the results.

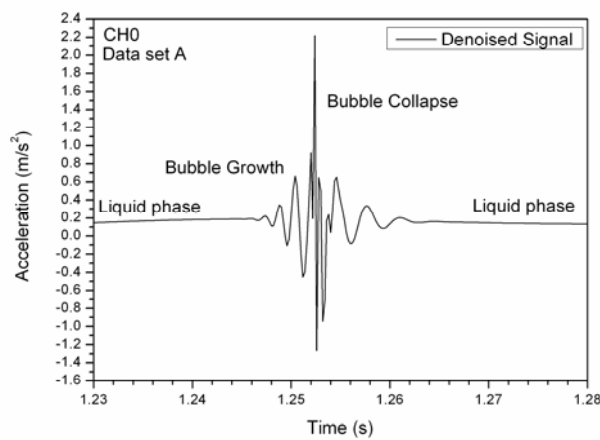


Fig. 9. Bubble growth and collapse captured after denoising of the acceleration data in the wavelet space. This signal refers to event number 1 notified on Fig. 8.

The spectrograms (Hanning window 512 samples, 64 frequency and 32 time bins) of the acceleration signal (CH0, Fig. 10) visualize almost instantaneous effects caused by bubbles collapsing near the walls. High power peaks in the full frequency domain indicate intensive vibrations of the mock-up window caused by forces induced by collapsing bubbles. Having known exact absolute time when the acquisition was started, it is easy to estimate the flow rate and the pressure in the system when this transient system behavior occurred. The Cavitation number is 2.5. The intensive developed cavitation has been started. The sudden change in a system behavior was successfully captured.

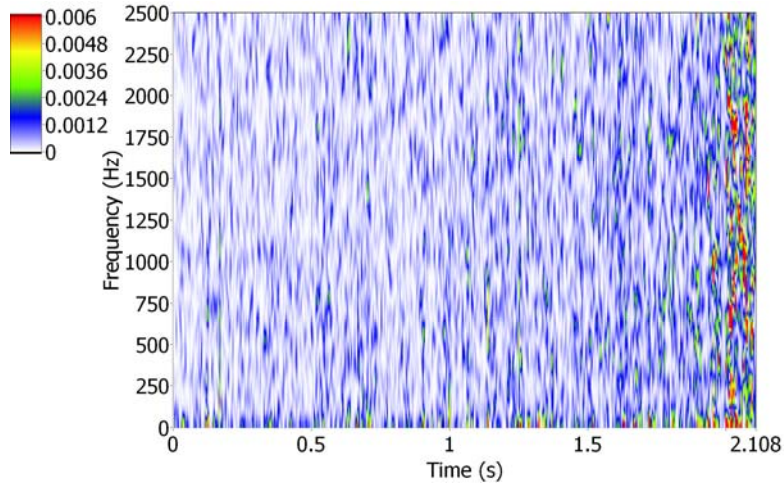


Fig. 10. Spectrogram of the STFT coefficients  $\left(\left(m/s^2\right)^2\right)$  for data set A.

#### 4.1.2. Sound pressure

In order to accompany above mentioned findings, an overview of sound pressure amplitudes for non-cavitating and cavitating flow regimes are compared in Fig. 11. Since the sound data are acquired with the personal computer at much higher sampling rates, the exact comparison of the absolute times is not possible. Anyway, incipient cavitation can be easily detected in the signal. The Cavitation number is 2.4. This regime is marked by window W1. Developed cavitation generates significant noise (window W2) i.e. amplitudes are much higher comparing to the non-cavitation regime. After the pressure of the cover gas is raised again and after all bubbles were collapsed the sound pressure is at the same level as at the beginning of the experiment (Window W3).

**ICANS XIX,**  
**19th Meeting on Collaboration of Advanced Neutron Sources**  
 March 8 – 12, 2010  
 Grindelwald, Switzerland

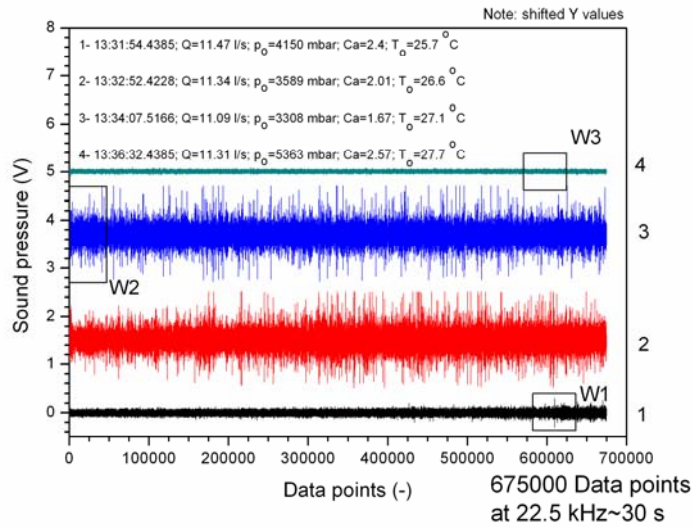


Fig. 11. Sound pressure data sets acquired for four characteristic regimes.

An example of transient data set acquired with LDV technique shows peaks in vibration data, which most probably means that several single bubbles collapsed. The acquisition was started at about 13:31:41. For comparison with acceleration data only first 8 s shown in Fig. 12 are of interest. The laser beam was pointed at the middle of the cusp window, which top penetrates into the liquid metal flow. The acceleration sensors captured developed cavitation a bit earlier at different location (concluded based on data shown in Fig. 10). The pressure of the cover gas was reduced from 3420 to 3220 mbar within 16 s, whereas the flow rate was kept constant at 11.04 l/s. The Cavitation number dropped below 2. The first peaks, which were registered in the signal after 2 s, have been detected in STFT spectrograms as well. They correspond to high frequencies between 175 and 250 kHz.

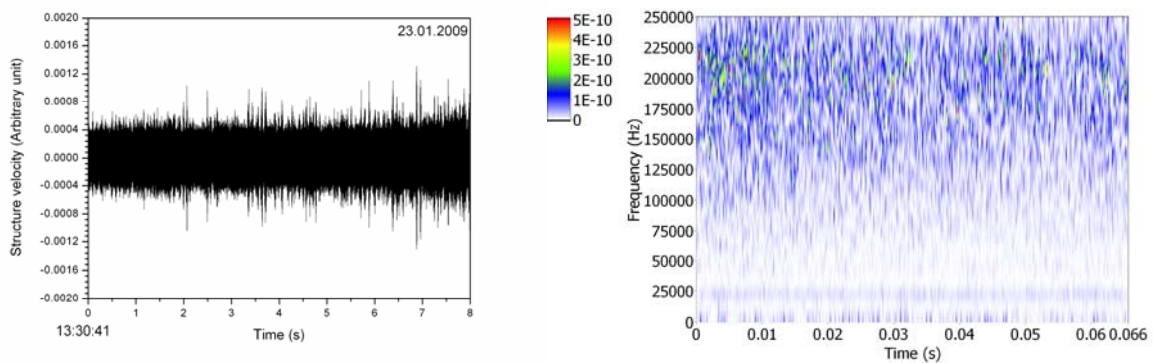


Fig. 12. The LDV data acquired at 0.5 MHz (left). The acquisition was started at 13:30:41. Spectrogram of the STFT coefficients ( $(m/s^2)^2$ ) show peaks in high frequency domain.

#### 4.2. Highlights of METEX 2 experimental session

During METEX 2 experiment special attention was given to pressure and acoustic emission measurements. Even though high-power peaks (see Fig. 13 and Fig. 14) confirmed existence of the distinct electromagnetic noise, the power level for no flow and for developed cavitation indicate clear enhancement in the lower frequency domain of the pressure signal

**ICANS XIX,**  
**19th Meeting on Collaboration of Advanced Neutron Sources**  
March 8 – 12, 2010  
Grindelwald, Switzerland

due to the cavitation and in the high frequency domain for the acoustic emission signal. Well-defined, broad acoustic emission power peak at  $10^5$  Hz (Fig. 13) for highest flow rate (10.92 l/s) and pressure of the cover gas 5550 mbar, indicated existence of cavitation. The Cavitation number was 3.5 and the temperature at the mock-up inlet was 28 °C. It must be also stressed that the data analyzed here refer to the second consecutive transient test. As developed cavitation was achieved in a previous run, pre-cavitation regime cannot be surely considered as a pure no-cavitation condition. Even though the Cavitation number was higher, the spectral power increase indicates developed cavitation.

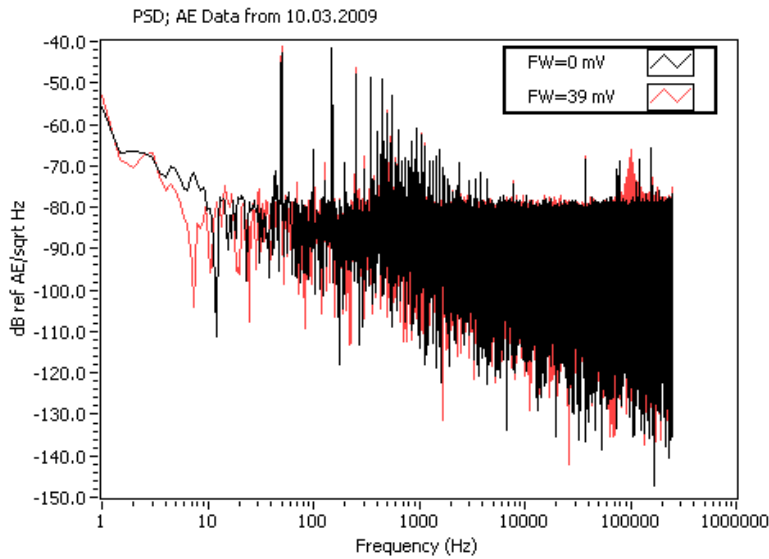
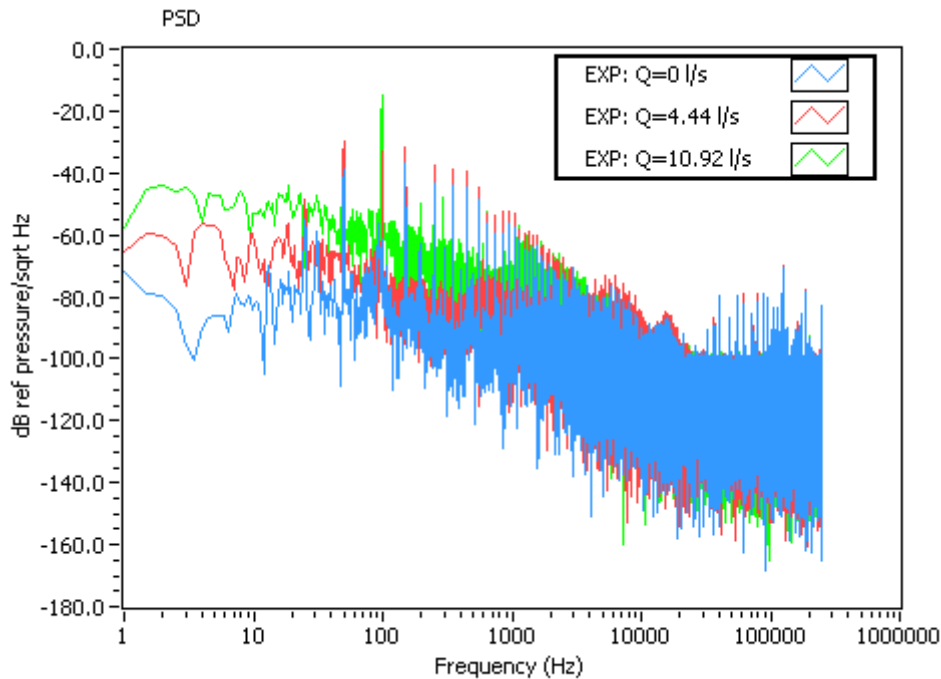


Fig. 13. Power Spectral Density of the acoustic emission data for no flow (FW=0 mV, FW is the pump output voltage) and for 11 l/s (FW=39 mV). Distinct peaks correspond to electromagnetic noise; whereas the power increment at about 200 kHz corresponds to the cavitation noise.



**ICANS XIX,**  
**19th Meeting on Collaboration of Advanced Neutron Sources**  
March 8 – 12, 2010  
Grindelwald, Switzerland

Fig. 14. Power Spectral Density of the acoustic emission data for no flow, 4.44 l/s and 11 l/s. Distinct peaks correspond to electromagnetic noise, whereas the power increase in a low frequency domain corresponds to the cavitation noise.

## 5. Conclusions

The experimental results presented here show that it was possible to detect incipient and developed cavitation during EURISOL mock-up testing. Since the cavitation phenomena cannot be observed in the liquid metal flows, these unique results provide the valuable information about the following:

- structural system behavior under hazardous cavitation flow regimes;
- signal patterns, which characterize incipient and developed cavitation in liquid metal flows;
- sensors, measurement locations and post-processing methods, which are successfully used to detect cavitation;
- comparisons of experimental results obtained from different sensors.

## References

1. Y. Blumenfeld and G. Fortuna, 2009. Final Report of the Eurisol Design Study (2005-2009), European Commission Contract No. 515768 RIDS, published by GANIL France. ([www.eurisol.org](http://www.eurisol.org))
2. Y. Blumenfeld on behalf of the EURISOL Design Study. EURISOL Design Study: Towards an Ultimate ISOL Facility for Europe, Invited talk at Franco-Japanese Symposium: New Paradigms in Nuclear Physics. Paris, France, Sept.29 - Oct.2 (2008)
3. S. Mallat. A wavelet tour of signal processing, ISBN: 978-0-12-466606-1 (1999)
4. R. Milenkovic, S. Dementjevs, K. Samec, E. Platacis, A. Zik, A. Flerov, K. Thomsen, Structural-hydraulic liquid metal test of the EURISOL target mock-up, Nuclear Instruments and Methods in Physics Research Section A, Vol. 607, Issue 2, pp. 279-292, (2009).
5. C. Kharoua, Y. Kadi, J. Lettry, L. Blumenfeld, K. Samec, K. Thomsen, S. Dementjevs, R. Milenkovic, A. Zik, E. Platacis and the Eurisol-DS task 2 collaboration, EURISOL-DS Multi-MW Target- Cavitation Detection by a Laser Doppler Vibrometer, CERN Eurisol-DS/Task2/TN-02-25-2009-0042, CERN (2009).

## Acknowledgement

The authors are grateful to August Kalt, Sergej Ivanov, Ernestas Platacis, Alexej Flerov and Anatolij Zik for their valuable assistance, numerous technical contributions to the design of the experimental installation and for carrying out the experiments. Valuable contributions to the test set-up, in particular to data acquisition, by Enzo Manfrin are gratefully acknowledged. Fillipo Barbagallo provided very useful ancillary equipment for placing thermocouples at the decisive locations. The authors are thankful to Knud Thomsen and Karel Samec for fruitful discussions, advices and support.

We acknowledge the financial support of the European Community under the FP6 ‘‘Research Infrastructure Action- Structuring the European Research Area’’ EURISOL DS Project Contract no. 515768 RIDS. The EC is not liable for any use that can be made on the information contained herein.